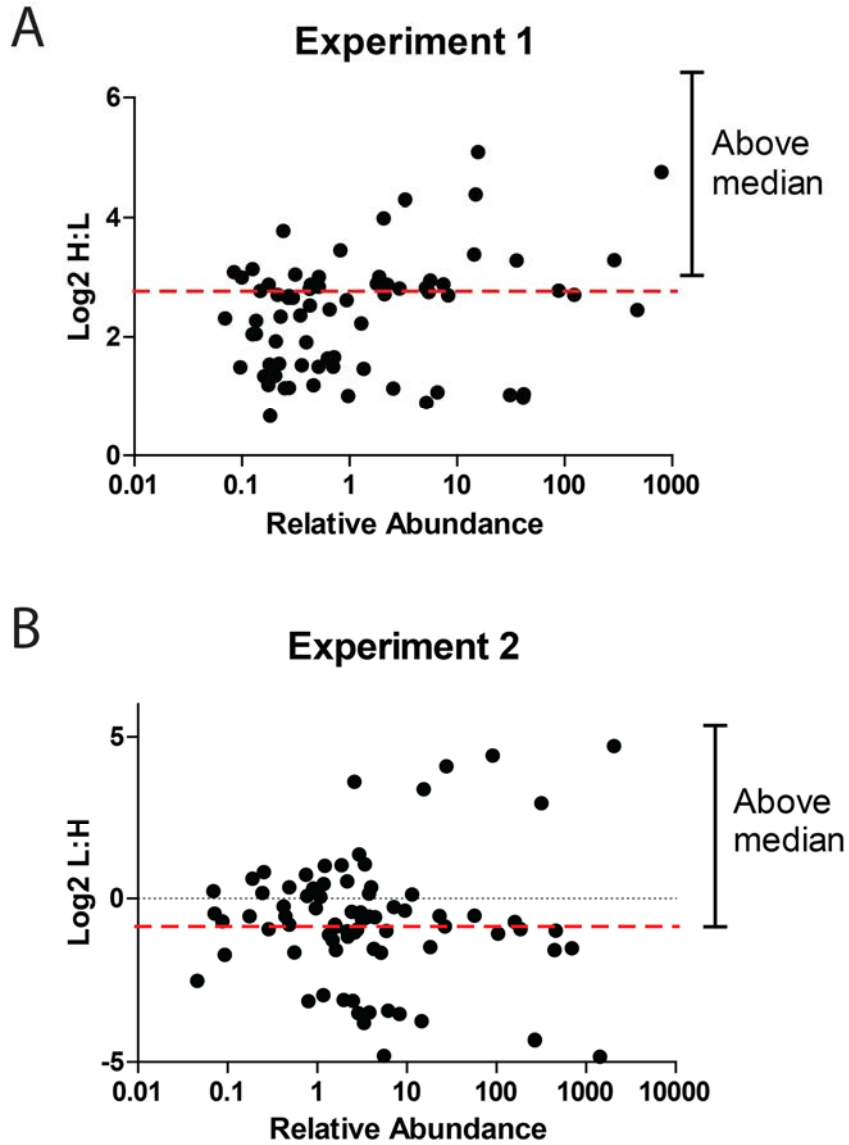


# Supplemental Materials

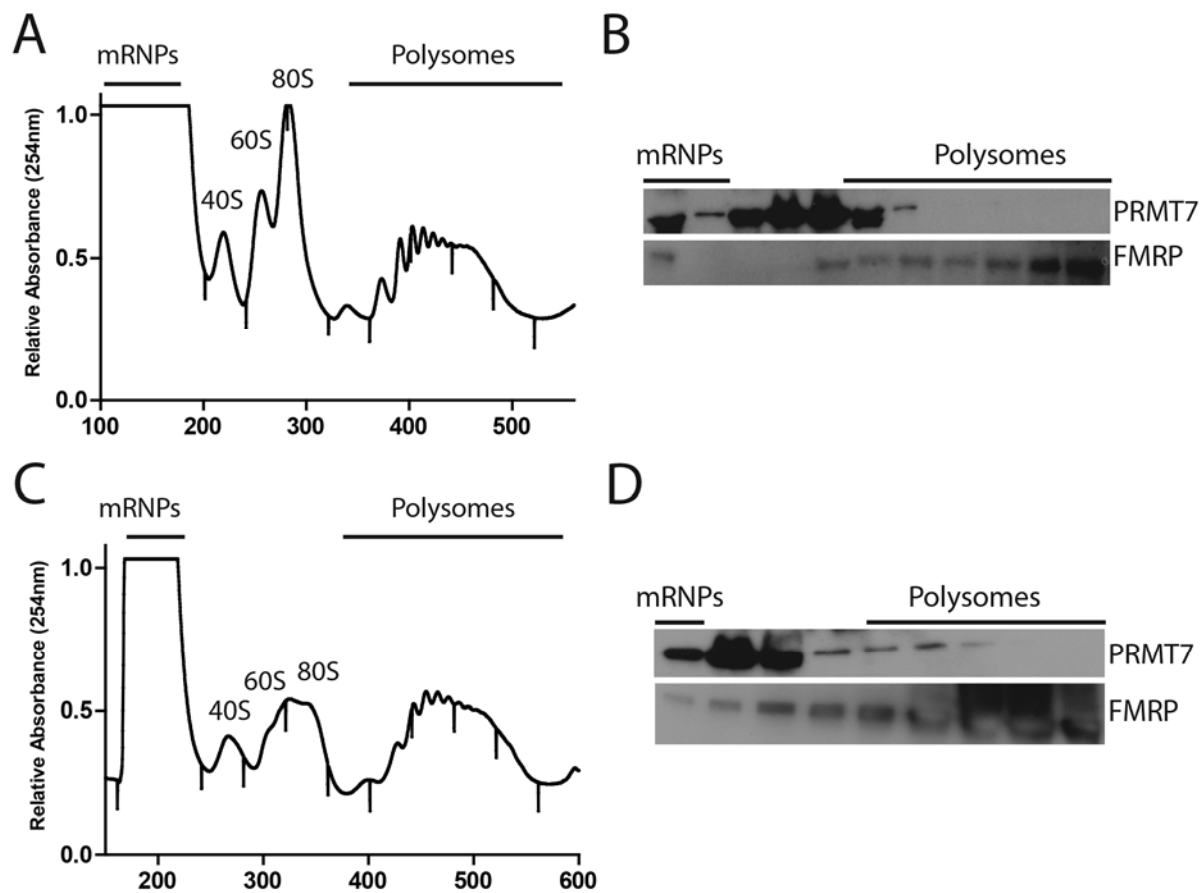
*Molecular Biology of the Cell*

Haghandish et al.



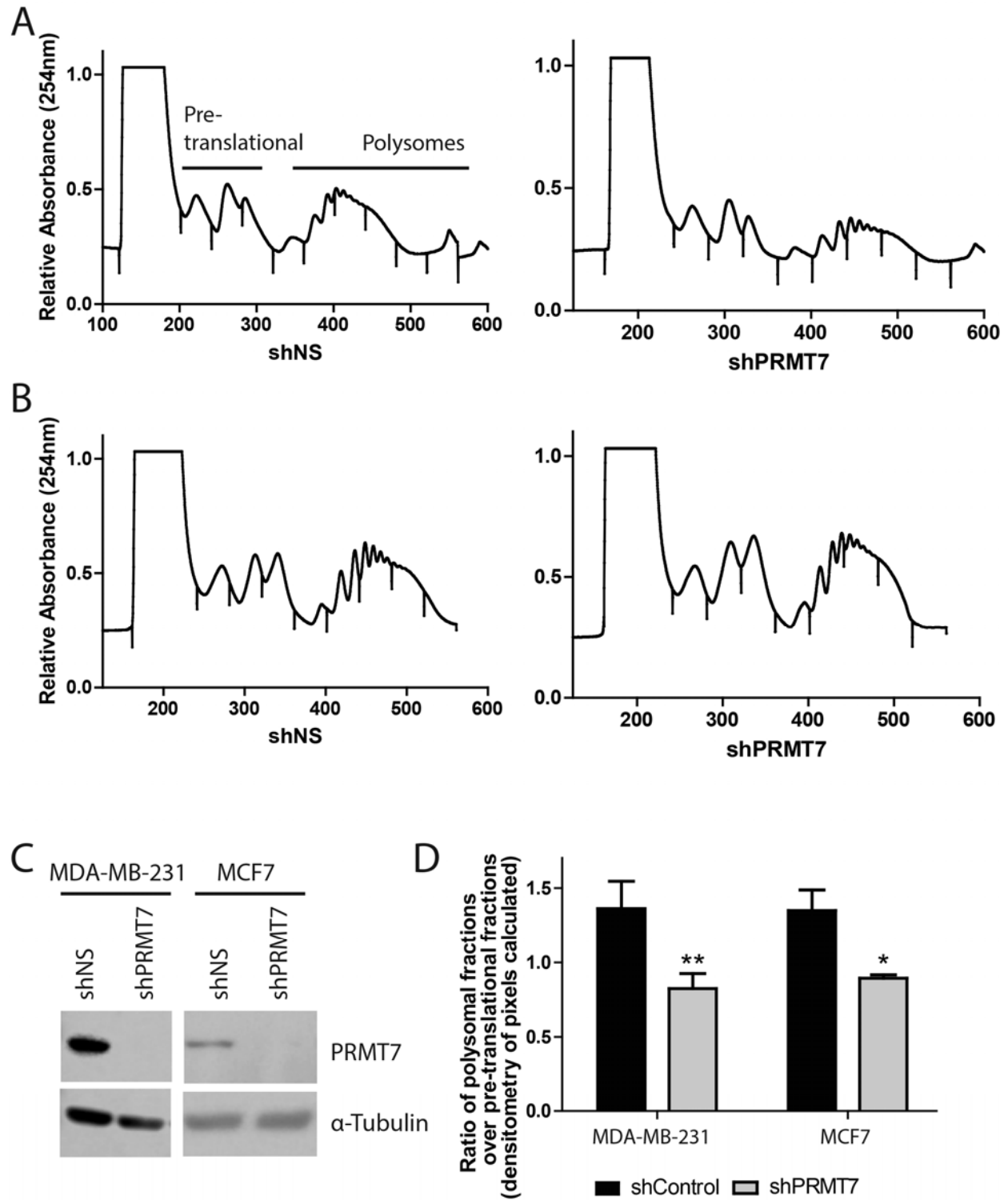
**Supplementary Figure 1**

**Supplemental Figure 1.** Analysis of SILAC-based mass spectrometry results. (A) Scatter plot showing comparison of the SILAC H:L ratio of proteins to their relative abundance within the mass spectrometry experiment (experiment 1). The median is marked by a dashed line. (B) Similar comparison but for experiment 2 (reverse labeling; SILAC ratio is L:H).



**Supplementary Figure 2**

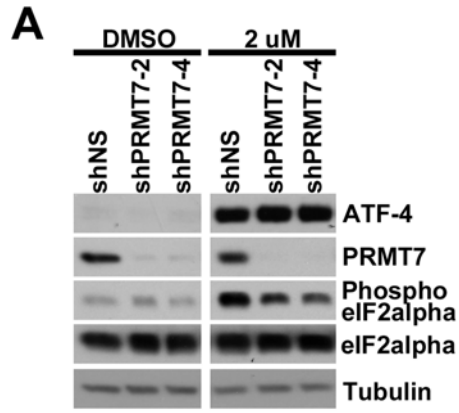
**Supplemental Figure 2.** PRMT7 is present in translational machinery within breast cancer cell lines. Polyribosome profiles and fractions of parental MCF7 cells (A, B) and parental MDA-MB-231 cells (C, D). Relative absorbance of RNA was read at 254nm. PRMT7 is found within both polysomes and pre-translational fractions – more so in cancer cells. FMRP was used as a positive control for pre-translational and polysomes.



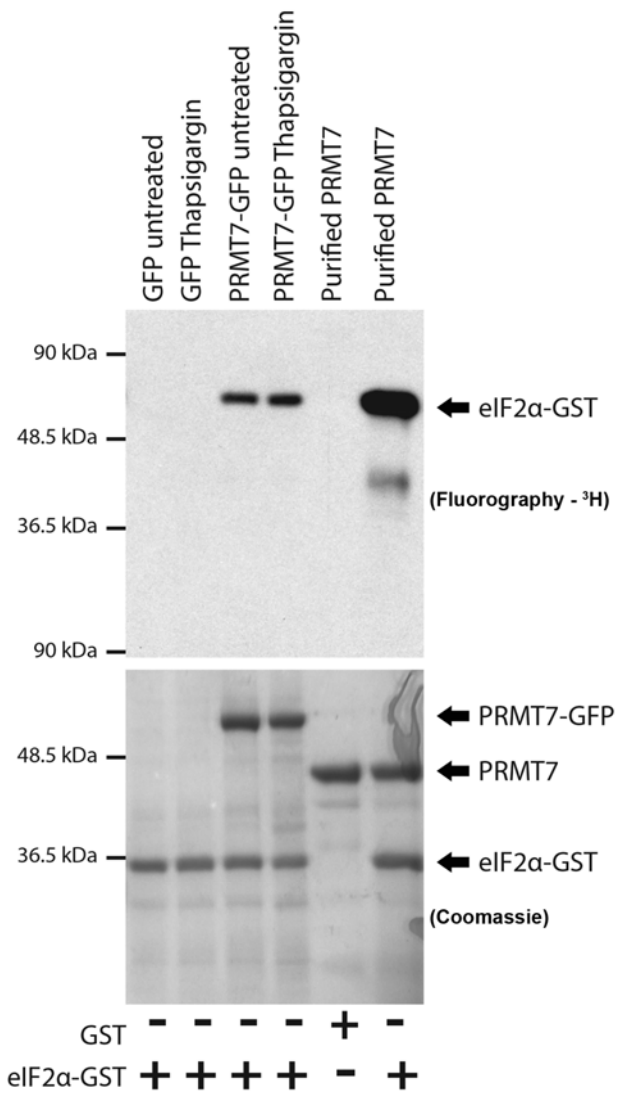
Supplemental Figure 3

**Supplemental Figure 3.** PRMT7 knockdown does not drastically affect polyribosome profile. (A) Representative polyribosome profiles of MDA-MB-231 cells 48 h post-infection with either control or PRMT7-targeting shRNAs. (B) Representative polyribosome profiles of MCF7 cells

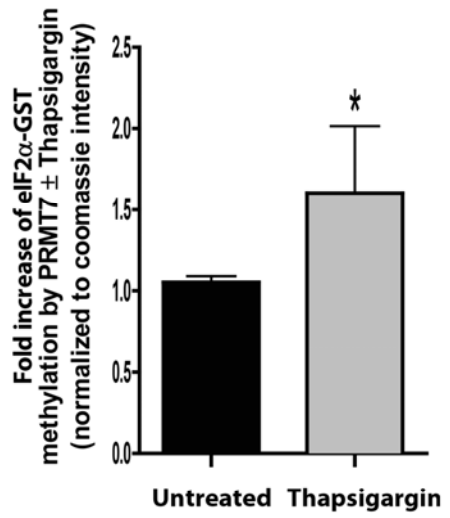
48 h post-infection with either control or PRMT7-targeting shRNAs. Relative absorbance of RNA was read at 254nm. (C) Western blots depict extent of PRMT7 knockdown in both cell types. (D) Quantification of the profiles revealed a statistically significant reduction of 36% in MDA-MB-231 cells and 32% s in MCF7 cells, upon PRMT7 knockdown (\*\*p=0.01; \*p=0.03, n=3, ANOVA; presented as mean  $\pm$  SEM).



**B** Immunoprecipitated using GFP-Trap beads

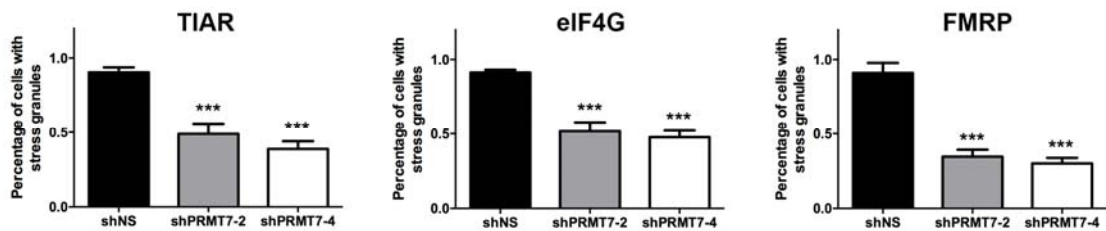
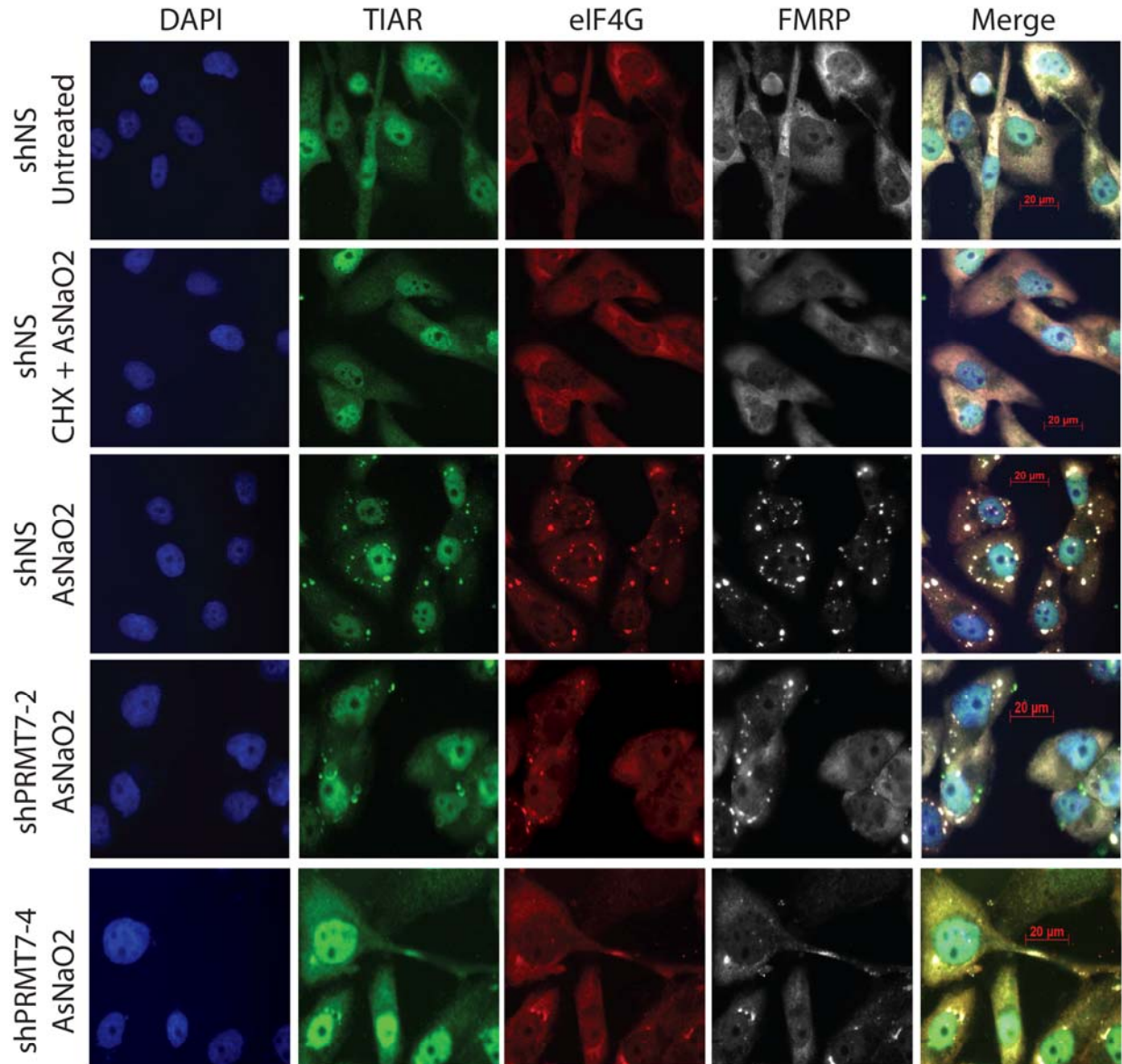


**C**



Supplemental Figure 4

**Supplemental Figure 4.** PRMT7 is more active, methylating eIF2 $\alpha$  to a higher degree, when cells are stressed with thapsigargin. (A) Accumulation of eIF2 $\alpha$  phospho-Ser51 following treatment with thapsigargin is reduced upon transient PRMT7 knockdown within MDA-MB-231 cells using two distinct shRNA targeting sequences. However, thapsigargin-induced accumulation of ATF4 is not affected upon PRMT7 knockdown. (B) PRMT7-Myc was transiently expressed in MDA-MB-231 cells and then affinity-purified using Myc-Trap beads. Affinity-purified PRMT7-Myc, from Mock- or thapsigargin-treated (2 $\mu$ M, 2 hours) was then used as a source of enzyme to perform *In vitro* methylation assays using <sup>3</sup>H-SAM as methyl-donor wild-type eIF2 $\alpha$ -GST as a substrate. Immunoprecipitated Myc was used as a negative control. As a positive control, purified PRMT7 with either GST or wild-type eIF2 $\alpha$ -GST was used. (C) Quantification of the methylation status of eIF2 $\alpha$  was calculated in the thapsigargin treated cells and normalized to the amount of PRMT7-myc detected in the coomassie stain. A significant increase in methylation of eIF2 $\alpha$  was observed in thapsigargin-treated cells; data are presented as mean  $\pm$  SEM for n=5, \*p=0.03, two-tailed t-test.

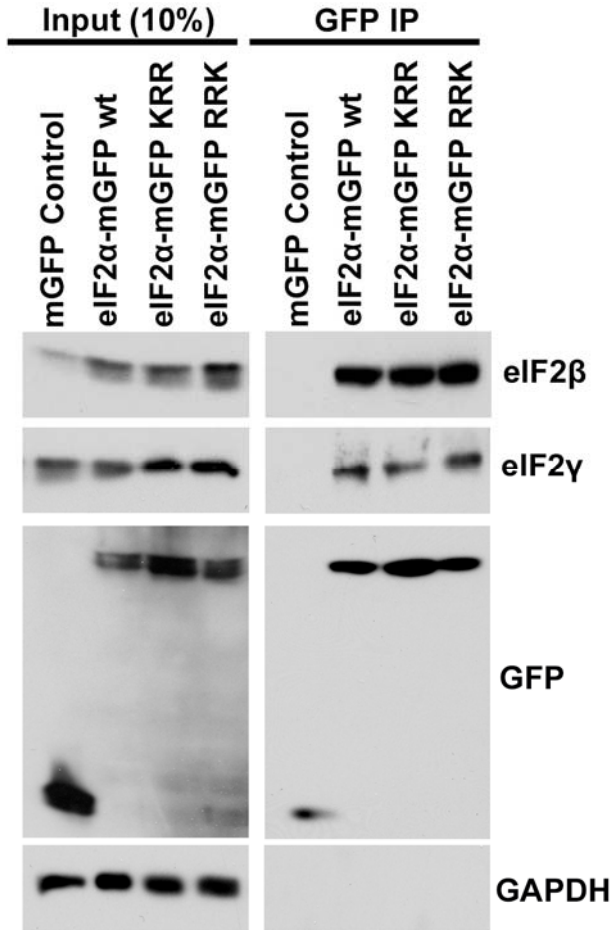


Supplemental Figure 5

**Supplemental Figure 5.** PRMT7 regulates stress granule formation. Representative immunofluorescent images of MDA-MB-231 cells depicting decreased stress granule formation upon transient knockdown of PRMT7 when exposed to AsNaO<sub>2</sub> (500μM for 30 minutes). Three stress granule markers were used: TIAR (green), eIF4G (red), and FMRP (white). Scale bar



20 $\mu$ m. Quantitation of stress granules from 3 independent experiments performed in triplicate when treated with AsNaO<sub>2</sub>; data are presented as mean  $\pm$  SEM, \*\*\*p=0.0001 (ANOVA). A cycloheximide control (CHX) was used to confirm the foci are stress granules as CHX prevents stress granule formation.



**Supplemental Figure 6.** Methylation of eIF2 $\alpha$  by PRMT7 does not affect its incorporation into the ternary complex. MDA MB 231 cells were infected with lentivirus expressing either EGFP, eIF2 $\alpha$ -mGFP wild type, KRR or RRR mutants. GFP-trap beads were used to affinity-purify EGFP and eIF2 $\alpha$  alleles from cell lysates, followed by immunoblotting for the eIF2 $\beta$  and eIF2 $\gamma$  subunits.